Received: 17 March 2020 | Revised: 28 July 2020 | Accepted: 28 September 2020

IET Communications

DOI: 10.1049/cmu2.12057

The Institution of Engineering and Technology WILEY

ORIGINAL RESEARCH PAPER

Low-complexity detection for uplink massive MIMO SCMA systems

Sanjeev Sharma[1] | **Kuntal Deka**[2] | **Baltasar Beferull-Lozano**[3]

[1] Indian Institute of Technology (BHU), Varanasi, India

[2] Indian Institute of Technology, Goa, India

[3] Department of Information and Communication Technology, University of Agder, Grimstad, Norway

Correspondence
Sanjeev Sharma, Indian Institute of Technology (BHU), Varanasi, India.
Email: tc2.sharma@gmail.com

Abstract

This paper presents a sparse code multiple access (SCMA) system with massive antennas at the base station. This system is referred to as M-SCMA system. A spectrally-efficient and massive access next-generation wireless network is realized through massive antennas and non-orthogonal SCMA techniques. Two detection algorithms, namely, modified message passing algorithm (MMPA) and extended message passing algorithm (EMPA) are proposed to detect multiple users' symbols in M-SCMA. A deep learning (DL)-based detection scheme is also proposed for M-SCMA so as to avoid channel estimation and to lower the detection complexity. Numerical results show that the DL-based detection has similar performance as MMPA even when the channel information is not estimated explicitly. Furthermore, authors also establish the sum rate trade-off between SCMA and orthogonal multiple access in a massive antenna system. The impact of various M-SCMA parameters such as the number of antennas and the overloading factor, on the proposed DL, MMPA, and EMPA-based detection are also investigated.

1 | INTRODUCTION

Recently non-orthogonal multiple access (NOMA) schemes are gaining interest for 5G and beyond wireless networks [1–6] NOMA-based systems have higher spectral efficiency than the orthogonal multiple access (OMA). Therefore, NOMA can support higher user density in next-generation wireless networks. Furthermore, multiple input and multiple output (MIMO) technology also increases spectral efficiency and/or improves wireless networks' performance. Upcoming wireless networks will be massive MIMO-based to enhance a system's performance [7–9]. Therefore, NOMA and MIMO will play a crucial role to design next-generation networks.

In the literature [1, 4, 10–15], NOMA techniques are categorized into two: power domain (PD) and code domain (CD). In CD-NOMA, the users occupy more than one orthogonal resources for communication and they are distinguished by different codewords. Examples for CD-NOMA include sparse code multiple access (SCMA) and pattern division multiple access (PDMA) methods. SCMA is more efficient than the PDMA due to high shaping and coding gain [16]. SCMA is gaining more interest than the PD-NOMA and PDMA [1]. Therefore, in this paper, we focus on the design and analysis of massive MIMO-based uplink SCMA system.

Related works: In [11], a beamforming technique is analysed for downlink NOMA system by considering the intra-beam interference in the system. However, [11] only focused on PD-NOMA based approach. In [10], a joint MIMO and SCMA detection is considered using message passing algorithm (MPA). However, the considered approach is analysed for only two antennas and has a very high complexity for large number of antennas. In [17], downlink SCMA capacity is analysed using multiple antennas, however, symbol error rate (SER) is not considered in [17]. In [18], spatial modulation SCMA system is analysed for small number of antennas. A space time block coding is also analysed in [19] for SCMA system. Furthermore, mostly work in MIMO-based NOMA systems are analysed for PD-NOMA in literature [20, 21]. Furthermore, some deep learning (DL)-based approaches are also analysed for SCMA system design [22, 23]. However, SCMA system with massive MIMO is not analysed by considering MPA or DL based detection method in SCMA literature. Therefore, it is interesting and useful to study a massive MIMO SCMA system by considering MPA or DL-based symbols detection.

Contributions: This paper proposes and analyses uplink massive MIMO SCMA system (referred to as M-SCMA system) Both SCMA and massive MIMO give higher throughput and improved system performance. The main contributions in the paper are summarized as follows:

- We propose DL-based detection for M-SCMA system. Since DL methods do not require channel information explicitly for data symbol detection and also has lower complexity as compared to conventional MPA-based detection.
- The deep neural network (DNN) model is trained offline from the simulated data, then it is used for online signal detection. The number of hidden layers and number of neurons at each layer are fixed in DNN by considering the multiple training to get a good SCMA system's performance.
- We propose a modified MPA (MMPA) to decode the data symbol in the proposed M-SCMA system. The MMPA offers receive beamforming gain at the base station (BS) for simple detection in M-SCMA. Furthermore, an extended MPA (EMPA) is proposed for M-SCMA to get both beamforming and detection gain. EMPA offers two contributions: (1) The min-sum approximation is used in lieu of the standard sum-product principle, and (2) the messages are damped in order to ensure correct convergence. The complexity of EMPA increases as the number of antennas increases at the BS as compared to MMPA. However, due to the min-sum approximation, the complexity of the detector reduces significantly. This point is further elaborated later in this paper.
- Analysis of the proposed M-SCMA system design in terms of bit error rate and the sum rate are carried out.
- The impact of M-SCMA system's parameters such as number of antennas and overloading factor are also analysed. Effect of imperfect channel information (ICI) is also studied in MMPA and EMPA-based detection since accurate channel information in M-SCMA is not practically viable [24].[1] Finally, we show numerical results to demonstrate the efficacy of MMPA, EMPA, and DL detection in the proposed M-SCMA system.

The rest of the paper is organized as follows. Section 2 introduces the proposed M-SCMA system model. Furthermore, DL, MMPA, and EMPA-based detection is also proposed in Section 2. Detection complexity is highlighted in Section 3. Numerical results and discussions are presented in Section 4. Finally, Section 5 concludes the paper.

Notations: $\mathcal{CN}(0, N_0\mathbf{I}_K)$ denotes the complex Gaussian distribution of zero mean and variance N_0 and $\mathbf{I}_K$ represents the identity matrix of size $K \times K$. $|\mathcal{B}|$ and $\|(\cdot)\|$ denote the cardinality of the set $\mathcal{B}$ and the Euclidean norm of a signal $(\cdot)$, respectively. $\mathbb{R}$ and $\mathbb{C}$ denote the real and complex numbers, respectively. The diag($\mathbf{h}$) represents the diagonal matrix corresponding vector $\mathbf{h}$ when elements of $\mathbf{h}$ are arranged in diagonal of the matrix.

[1] Accurate channel information in M-SCMA needs complex processing due to non-orthogonal nature of system.

2 | PROPOSED M-SCMA SYSTEM MODEL

In this section, M-SCMA-based communication system is proposed to enhance the system's capacity and detection performance. Uplink M-SCMA system has J users and K orthogonal resources with $J > K$ and referred as $J \times K$ M-SCMA system. In M-SCMA, each user has single antenna and the BS is equipped with Z antennas, as shown in Figure 1. Let jth user information symbol and codebook are denoted as d_S^j and $\mathcal{X}_j, j = 1, 2, \dots, J$, respectively. Symbol d_S^j can take one value from the M possible values at a time, i.e. $d_S^j \in \mathcal{D} = \{d_{S,1}^j, \dots, d_{S,M}^j\}$ with $|\mathcal{D}| = M$. Since in SCMA, each symbol is mapped to K-dimensional complex codeword [4, 5]. Therefore, a codebook of each user has M complex valued columns and is denoted as $\mathcal{X}_j \in \mathbb{C}^{K \times M}$. Furthermore, each column of $\mathcal{X}_j$ has only N ($N < K$) non-zero elements out of K. Therefore, codebooks $\{\mathcal{X}_j\}s$ are sparse in SCMA system. The channel impulse response (CIR) between jth users and zth antenna at BS is denoted as $\mathbf{h}_{j,z} \in \mathbb{C}^K, z = 1, 2, \dots, Z$. Received signal $\mathbf{y}_z = (y_{z1}, \dots, y_{zK}) \in \mathbb{C}^K$ at the zth antennas can be expressed as

$$\mathbf{y}_z = \sum_{j=1}^{J} \sqrt{P_j}\,\mathrm{diag}\big(\mathbf{h}_{j,z}\big)\mathbf{x}_j, \tag{1}$$

where P_j and $\mathbf{x}_j \in \mathcal{X}_j$ represent the transmit power and codeword of jth user, respectively. The jth user symbol detection using maximum a posteriori (MAP) probability is written as

$$\hat{\mathbf{x}}_j = \arg\max_{\mathbf{x_j} \in \mathcal{X}_j} \sum_{\mathbf{x}_l \in \mathcal{X}_l \forall l \neq j} p(\mathbf{x}_l | \{\mathbf{y}_1, \mathbf{y}_2, \dots, \mathbf{y}_Z\}), \tag{2}$$

where $p(\mathbf{x}_l|\{\mathbf{y}_1, \mathbf{y}_2, \dots, \mathbf{y}_Z\})$ denotes the a posteriori probability of the lth user given all the antennas' received signal $\{\mathbf{y}_1, \mathbf{y}_2, \dots, \mathbf{y}_Z\}$. Computational complexity of the MAP-based detection in (2) is high and it increases exponentially as number of users and antennas increase in the system [4, 5]. Therefore, we propose a DNN-based receiver for M-SCMA system below.

2.1 | DNN-based detection

In general, MPA-based detection is used for data symbol detection in SCMA. MPA-based detection requires exact CIR of each user at the BS. However, the exact CIR of users is not available in practice or complex to estimate in NOMA uplink systems. Therefore, we proposed a DL-based symbols detection in the uplink M-SCMA system. DL-based symbol detection does not require the explicit channel information [25–29], and it learns the joint effect of CIR and signal detection.

A neural network (NN) maps the received signal to the data symbols and expressed as [30]

$$f(\mathbf{\Theta}, \mathbf{y}_t) : \mathbf{y}_t \rightarrow \hat{D} = \{d_{S,t}^1, d_{S,t}^2, \dots, d_{S,t}^J\}, \tag{3}$$

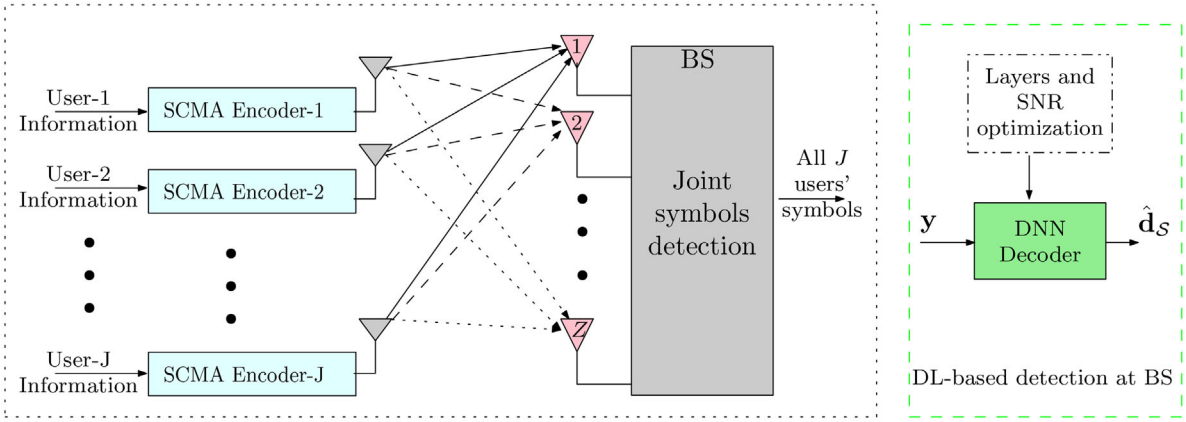

FIGURE 1 System model of the proposed uplink M-SCMA

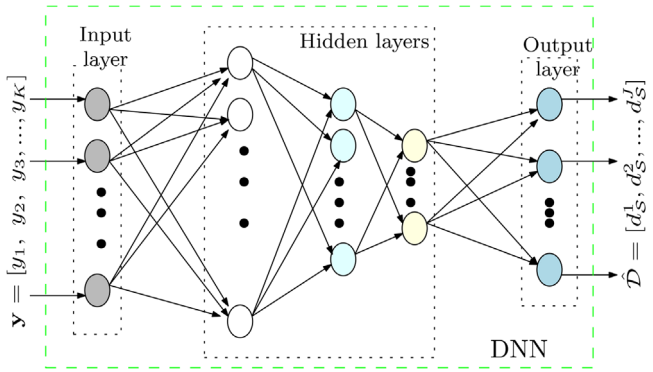

FIGURE 2 DNN with L hidden layers and each layer has $\mathcal{L}_l, l = 1, 2, \ldots, L$ neurons

where $\mathbf{y}_t$ is the received signal at BS in tth time frame, and $d_{S,t}^j$ is the jth user symbol in tth time frame. $\boldsymbol{\Theta}$ is a DNN parameter, which needs to learn during the offline training of DNN. Therefore, DNN function $f(\boldsymbol{\Theta}, \mathbf{y}_t)$ should be learned from the data set so that error probability of symbol detection is minimized.

2.1.1 | DNN offline training

DNN consists of input, output, and multiple hidden layers, where each layer has multiple neurons [28–30], as shown in Figure 2. Each neuron maps weighted sum of inputs form the previous layer to the output using non-linear activation function. The mostly used non-linear activation functions can be Relu, sigmoid, hyperbolic tangent etc., and are defined as

$$f_{\text{relu}}(q) = \max\{0, q\} \quad f_{\text{sig}}(q) = \frac{1}{1 + \exp(-q)}, \quad \text{and} \quad f_{\tanh}(q) = \frac{\exp(q) - \exp(-q)}{\exp(q) + \exp(-q)}. \tag{4}$$

The layers in the DNN are cascaded to generate the final output as shown in Figure 2. Hence, decoder output is expressed as

$$\hat{\mathcal{D}} = \mathbf{y}_L = f(\boldsymbol{\Theta}, \mathbf{y}_1) = f^L(f^{L-1}(\ldots f^1(\mathbf{W}_1\mathbf{y}_1 + \mathbf{b}_1))), \tag{5}$$

where L is the total number of layers in the DNN. The $\mathbf{y}_1$ is the input vector, and $\mathbf{W}_l$ and $\mathbf{b}_l$ are weight and bias vector at the lth layer, $l = 1, 2, \ldots, L$. The parameter $\boldsymbol{\Theta} = \{\mathbf{W}_L, \ldots, \mathbf{W}_1, \mathbf{b}_L, \ldots, \mathbf{b}_1\}$ consist of weight and bias variance. Furthermore, DNN parameter $\boldsymbol{\Theta}$ is optimized by minimizing the $\mathcal{L}_2$ loss function and it is expressed as

$$\mathcal{L}_2 = \frac{1}{\mathcal{N}_1} \sum_{k} ||\hat{\mathcal{D}}(k) - \mathcal{D}(k)||_2, \tag{6}$$

where $\mathcal{D}(k)$ and $\hat{\mathcal{D}}(k)$ are the transmit (during training) and estimated data symbols, respectively. Therefore, $\boldsymbol{\Theta}_{\text{opt}} = \min_{\boldsymbol{\Theta}}\{\mathcal{L}_2\}$.

Furthermore, a priori domain knowledge (if available) can prescribe the choice of a specific hypothesis class for use in the training process, which results in an efficient and effective DNN training in the system. Let training set $\mathcal{T}$ consists of $\mathcal{N}_1$ frames with training points $(\mathbf{y}_{n_1}, \mathcal{D}_{n_1})$, $n_1 = 1, \ldots, \mathcal{N}_1$, where $\mathbf{y}_{n_1}$ and $\mathcal{D}_{n_1}$ the received signal and corresponding output data symbols (of all users) in the n_1th frame. In the DL-based decoder, aim to derive a predictor $\zeta(\mathbf{y})$ from the training data set $\mathcal{T}$ that generalize the input-output mapping to the inputs $\mathbf{y}$ that is not present in $\mathcal{T}$. Therefore, DL-based decoder predict output $\mathcal{D}$ from the posterior distribution

$$\mathcal{P}(\mathcal{D}|\mathbf{y}) = \frac{\mathcal{P}(\mathbf{y}, \mathcal{D})}{\mathcal{P}(\mathbf{y})} \tag{7}$$

by minimizing the loss function $\mathcal{L}_2$. In (7), $P(\mathbf{y}, \mathcal{D})$ and $\mathcal{P}(\mathbf{y})$ denote the joint and marginal distribution, respectively. The optimal predictor $\zeta(\mathbf{y})$ for any received signal $\mathbf{y}$ is expressed as

$$\zeta(\mathbf{y}) = \arg\min_{\mathcal{D}} E_{\mathcal{D}\sim\mathcal{P}(\mathcal{D}|\mathbf{y})}[\mathcal{L}_2|\mathbf{y}]. \tag{8}$$

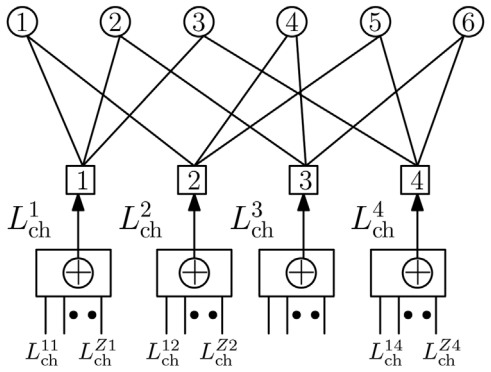

FIGURE 3 Calculation of channel LLR in MMPA-based detection

Therefore, an optimal predictor $\zeta(\mathbf{y})$ is obtained by minimizing the average loss $\mathcal{L}_2$ for output value $\mathcal{D}$, where the average is evaluated with respect to the posterior distribution $\mathcal{P}(\mathcal{D}|\mathbf{y})$ [28].

2.2 | MPA-based detection

In this subsection, we propose MPA (MMPA)-based detection for the M-SCMA system. The factor graph of M-SCMA system is modified to use MPA for symbol detection and is described below.

2.2.1 | MMPA-based detection

We propose MMPA-based detection for the M-SCMA. Consider the uplink system model shown in Figure 1 where there are J users with single antenna each and one BS with Z antennas. The signal $\mathbf{y}_z = [y_{z1}, y_{z2}, \ldots y_{zK}]^T$ received by the zth antenna at the BS is given by

$$\mathbf{y}_z = \sum_{j=1}^{J} \sqrt{P_j}\,\mathrm{diag}\left(\mathbf{h}_{j,z}\right)\mathbf{x}_j + \mathbf{w}_z, \tag{9}$$

where $\mathbf{w}_z$ is the additive white Gaussian noise (AWGN) at the zth antenna and is distributed as $\mathbf{w}_z \sim \mathcal{CN}(0, N_0\mathbf{I}_K)$.

The message passing procedure in MMPA can be carried out either in probability domain log-likelihood ratio (LLR) domain. However, LLR-domain implementation is preferable in hardware due to numerical stability. Suppose the channel LLR computed from y_{zk} is denoted by L_{ch}^{zk}. The effective channel LLR L_{ch}^{k} received by the kth resource node is given by

$$L_{ch}^{k} = \sum_{z=1}^{Z} L_{ch}^{zk}. \tag{10}$$

The procedure of MMPA is illustrated in Figure 3. Here, the factor graph remains the same as in the single-input single-output (SISO) case The input channel LLR to a resource node combines the channel LLRs from all the antennas in an equal-gain-combining fashion. Then the normal steps for MPA are carried out to extract the multiple users' data.

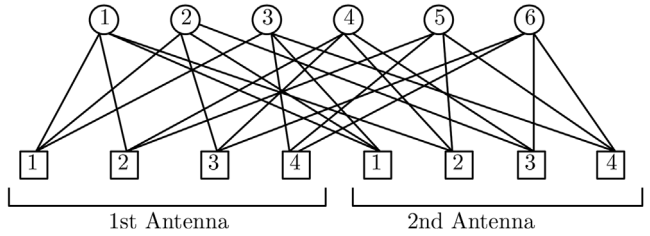

FIGURE 4 Extended factor graph for 6×4 M-SCMA system with $Z = 2$

2.2.2 | EMPA-based detection

Simple receive beamforming based M-SCMA system does not utilize the all antennas' signal effectively to improve performance since conventional $J \times K$ SCMA detection is used at the BS. In this subsection, we propose an EMPA to get both beamforming and detection gain in M-SCMA system. The received signal by concatenating all the antennas's signal in a vector form is written as

$$\mathbf{y}_E = [\mathbf{y}_1^T, \mathbf{y}_2^T, \ldots, \mathbf{y}_Z^T]^T \in \mathbb{C}^{ZK\times 1} \tag{11}$$

and jth user channel matrix is given as

$$\mathbf{H}_{E,j} = \begin{bmatrix} \mathrm{diag}\left(\mathbf{h}_{j1}\right) & 0 & \cdot & 0 \\ 0 & \mathrm{diag}\left(\mathbf{h}_{j2}\right) & 0 & 0 \\ \vdots & \vdots & \ddots & \cdot \\ \cdot & \cdot & 0 & \mathrm{diag}\left(\mathbf{h}_{j,Z}\right) \end{bmatrix} \tag{12}$$

of size $ZK \times ZK$. Therefore, the received signal is expressed as

$$\mathbf{y}_E = \sum_{j=1}^{J} \sqrt{P_j}\mathbf{H}_{E,j}\mathbf{x}_{E,j} + \mathbf{w}_E, \tag{13}$$

where $\mathbf{x}_{E,j} = [\mathbf{x}_j^T, \mathbf{x}_j^T, \ldots, \mathbf{x}_j^T] \in C^{ZK\times 1}$ and $\mathbf{w}_E = [\mathbf{w}^T, \ldots, \mathbf{w}^T] \in C^{ZK\times 1}$.

The modified factor graph by combining all antennas' signal in EMPA is expressed in Figure 4 for $Z = 2$. Observe that the extended factor graph contains six user nodes as each user is having only one antenna. The number of resource nodes in the extended factor graph is equal to $2 \times 4 = 8$ as there are $Z = 2$ antennas in the BS. Observe that the degree of the resource node is the same as $d_f = 3$. However, the degree of a user node increases from 2 to 4. This implies that a user gets higher number of opinions regarding its value. This results in the increase in the detection diversity. Due to this, the EMPA can yield impressive performance.

In EMPA, we offer two contributions which reduce the overall complexity of the detection process. First, the calculation of

the messages from the factor nodes are simplified by considering the min-sum approximation. The decoding is represented in the LLR domain. A message is proportional to the negative logarithm of the likelihood. The min-sum approximation is similar to the one considered in the context of the decoding for non-binary low-density parity-check (LDPC) codes [31] Suppose $\{\mathbf{V}_{ji}\}_{j=1}^{j=d_f}$ denote the messages coming to the ith factor node from the d_f neighbouring user nodes. The message $\mathbf{U}_{ij}$ from the ith factor node to the jth user node is updated as per the min-sum approximation:

$$U_{i\to j}(\mathbf{x}_{jm}) = \min\left(L_{\mathrm{ch}_j} + \sum_{\substack{j'=1 \\ j'\neq j}}^{d_f} \mathbf{V}_{j'i}\right), \tag{14}$$

where the minimum value is obtained among all combinations of the symbols for all the neighbouring user nodes except for the jth one. In (14), the symbol for the jth user node is fixed at $\mathbf{x}_{jm}$.

The second contribution in EMPA is the damped update of the messages. The message $U_{i\to j}^{(l)}(\mathbf{x}_{jm})$ at the lth iteration is updated as per the following equation:

$$U_{i\to j}^{(l)}(\mathbf{x}_{jm}) = \alpha U_{i\to j}^{(l)}(\mathbf{x}_{jm}) + (1-\alpha)U_{i\to j}^{(l-1)}(\mathbf{x}_{jm}), \tag{15}$$

where $\alpha \in (0, 1)$ is the damping factor. The damped update in (15) is carried out for every message in the EMPA. The damping ensures that the EMPA does not diverge and converges to a correct solution.

3 | DETECTION COMPLEXITY

EMPA operates over the extended factor graph. Observe from Figure 4 that the degree d_f of the resource node is the same as that for the MMPA. The complexity depends on the number of bits per symbol, i.e. M and overlapping users at each resource node, i.e. d_f, and is expressed as $O(M^{d_f} + \mathcal{F})$, where $\mathcal{F}$ depends on the M, K, and d_f. However, factor M^{d_f} dominates the complexity. Therefore, for I iterations, the complexity is expressed as $I \times O(M^{d_f})$. The min-sum approximation is considered in EMPA. It offers a nice advantage that the signal-to-noise ratio (SNR) estimation is no longer required Moreover, observe from (14) that we need to find only the minimum value among M^{d_f} terms instead of summing all these terms. This approximation reduces the implementation overhead significantly.

DNN is trained offline using a training data set, hence it does not include the training complexity while it uses for online data symbols detection. Considering a well-trained fully connected DNN model, for each data transmission/reception, the online training complexity depends on the number of vector-matrix multiplication. DNN's complexity is $L_1N + L_1L_2 + L_2L_3$ vector-matrix multiplication, where L_i denote the active parameters in all neurons in each hidden layer and N be the number of DNN inputs. Furthermore, modulation order and d_f have almost zero effect on the detection time in DNN-based decoder. Therefore, DNN-based decoder has lower complexity as compared to the MPA-based decoder.

4 | SIMULATION RESULTS AND DISCUSSION

In this section, we present the performance of the proposed M-SCMA system using the MMPA, EMPA, and DL-based detection algorithms. The uncoded transmission over Rayleigh fading channels are used. The average SER and sum rate performance metrics are considered for analysis.

4.1 | System parameters

The M-SCMA system, with $K = 4$ orthogonal resources and $J = 6, 8, 12$ users, is considered. These parameters result in overloading factors of $\lambda = K/J = 1.5, 2, 3$. Number of antennas Z at the BS are considered in the range of 1–100. The codebooks of users are generated using the methods in [16, 32, 33]. Furthermore, we also assume each user's codebook is normalized to unity and uses two bits per symbol for transmission, i.e. $|\mathcal{D}| = M = 4$. DNN at the BS is trained offline generating stochastic data, while online detection is used for considering the independent data set in the M-SCMA system. All the users have same transmitted power and one unit power per user is used in numerical results.

4.2 | DNN parameters

This paper considered input, output, and three hidden layers in the DNN for data symbol detection. The $\mathcal{L}_1 = 380$, $\mathcal{L}_2 = 10$, and $\mathcal{L}_3 = 10$ neurons are considered at the first, second, and third hidden layers, respectively. The Sigmoid non-linear activation functions is used on hidden layers in DNN with the linear function on the output layer. The 1000 epochs and learning rate $\alpha = 0.01$ are used with the steepest descent algorithm optimization [22] method in the DNN training. The DL decoder is trained by considering randomly generated data symbols over flat Rayleigh fading wireless channel by considering as a black-box. Furthermore, the received signal corresponding the $\mathcal{N}_1 = 10,000$ transmitted data symbols are used in DNN training at SNR=20 dB[2] since it leads to the optimal SER performance over the entire SNR range.

[2] After training the DNN at different SNR and hidden layers, we get the best M-SCMA performance for considered parameters.

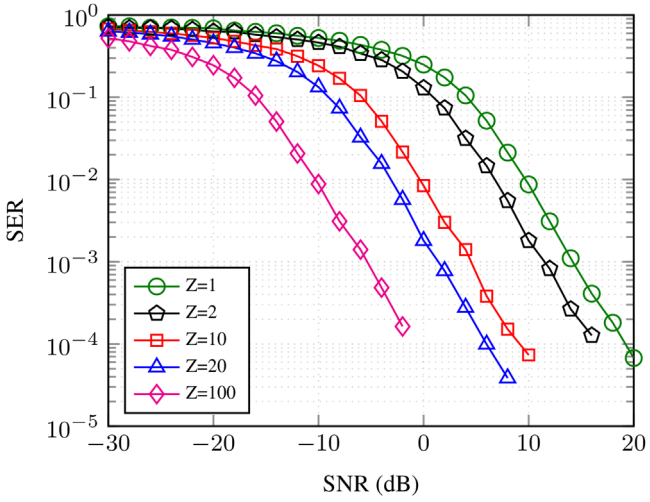

FIGURE 5 SER performance of the proposed 6 × 4 M-SCMA system in Rayleigh channel using the proposed MMPA

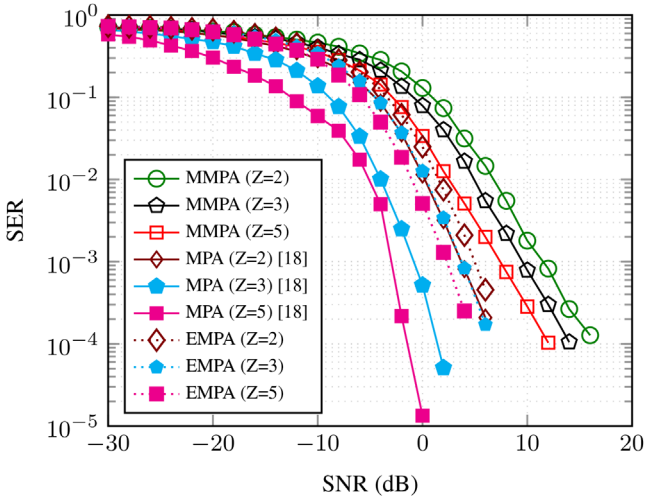

FIGURE 6 SER performance of the proposed 6 × 4 M-SCMA system in Rayleigh channel using the proposed MMPA and EMPA

4.3 | Simulations results

The average SER of 6 × 4 M-SCMA system is shown in Figure 5 for different number of antennas at the BS. As the number of antennas Z increases at BS, array gain of the proposed M-SCMA system also increases, as observed in Figure 5. Therefore, M-SCMA can achieve higher energy and spectral efficiency due to multiple antennas at BS and non-orthogonal SCMA, respectively.

Average SER performance of M-SCMA using the proposed MMPA and EMAP is shown in Figure 6. The MMPA has only SNR gain since it uses only beamforming at the BS as observed in Figure 6. The EMPA has both SNR and decoding gain as shown in Figure 6 due to the large factor graph is used in detection. Furthermore, decoding gain is more prominent for large number of receiver antennas over SNR gain in Figure 6. However, EMPA has higher complexity (marginally)

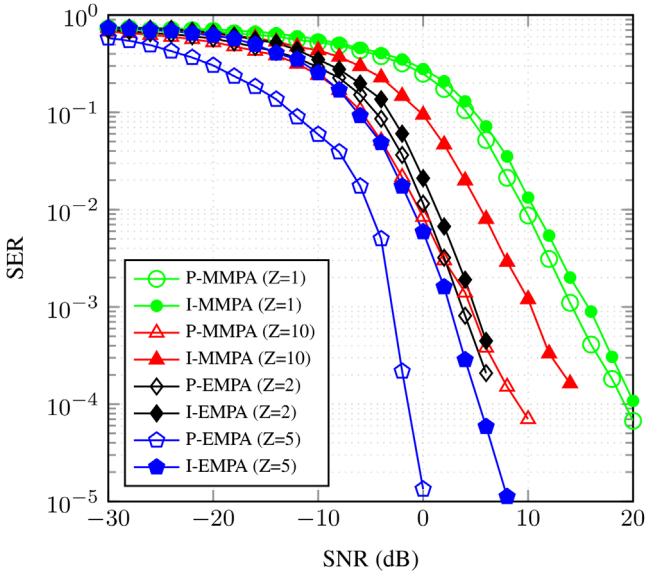

FIGURE 7 Impact of imperfect CIR on MMPA and EMPA detection

as compared to the MMPA. Furthermore, conventional MPA [18] has improved performance as compared the proposed MMPA and EMPA, as observed in Figure 6 with increased complexity.

4.3.1 | Impact of imperfect CIR

The proposed MMPA and EMPA-based symbol detection require perfect channel state information of each user. The received signal is the superposition of each users' data symbol and their channel information in the M-SCMA system. Therefore, accurate CIR estimation at the BS is either complex or impossible due to non-orthogonal pilots. Thus, MMPA and EMPA detection is analysed for ICI scenario in Figure 7. The actual CIR $\mathbf{h}_{jz}$ and estimated CIR $\bar{\mathbf{h}}_{jz}$ are related for zth received antenna and jth user as

$$\mathbf{h}_{jz} = \bar{\mathbf{h}}_{jz} + \mathbf{e} \in \mathbb{C}^K, \quad j = 1, \dots, J, z = 1, \dots, Z, \tag{16}$$

where $\mathbf{e}$ is the estimation error between actual CIR $\mathbf{h}_{jz}$ and estimated CIR $\bar{\mathbf{h}}_{jz}$. Error $\mathbf{e}$ can be modelled as a complex Gaussian random vector with zero mean and the covariance matrix $\sigma_e^2\mathbf{I}_K$, where $\mathbf{I}_K$ is the $K \times K$ identity matrix. Furthermore, σ_e^2 linearly decreases with increasing SNR [26]. In Figure 7, $\sigma_e = 0.3/\text{SNR}$ is used by considering the CIR norm is unity. Impact of ICI increases as the number of antennas increases at the BS, as observed in Figure 7 for both MMPA and EMPA detection. We observe that SER performance degrades around 7dB at SER $= 10^{-4}$ for both MMPA ($Z = 10$) and EMPA ($Z = 5$) in ICI scenario (denoted as 'I') as compared to the perfect CIR (denoted as 'P'), as observed in Figure 7. Hence, a large number of antennas at BS only benefit M-SCMA system in a perfect CIR scenario for both MMPA and EMPA-based detection.

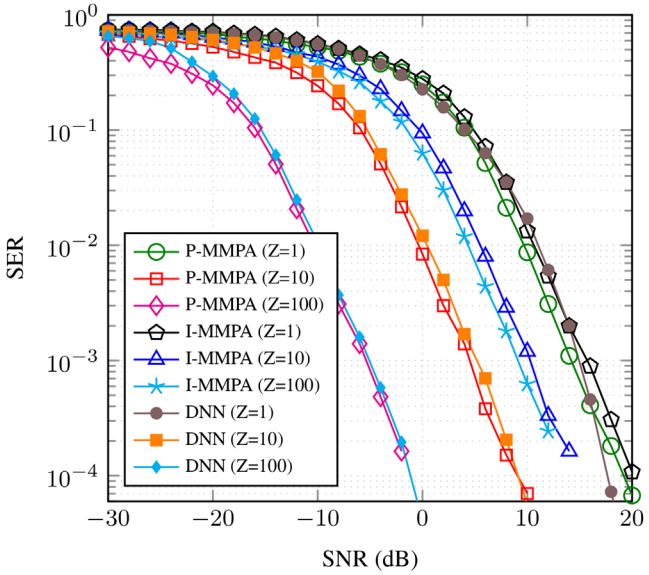

FIGURE 8 DNN and MMPA-based symbol detection in the M-SCMA system

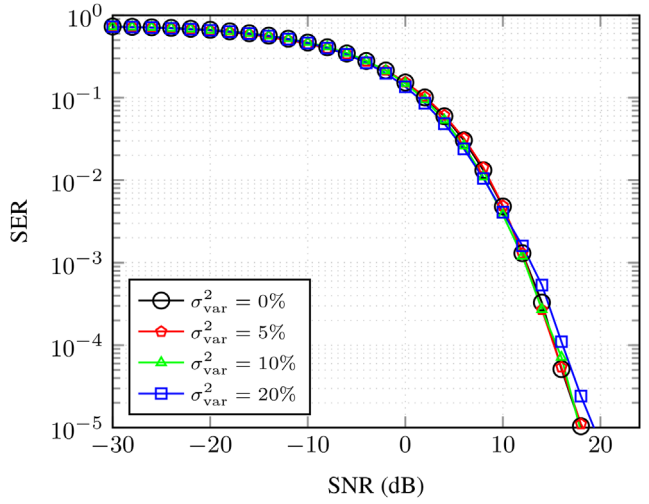

FIGURE 9 Average SER performance with channel statistics mismatches between offline training and online testing with $Z = 5$

4.3.2 | DNN detection

Furthermore, the proposed M-SCMA's SER performance using DNN detector is shown in Figure 8. DNN has close performance to the MMPA-based detection (with perfect CIR), as observed Figure 8. However, DNN outperforms than the MMPA in ICI scenarios.

Robustness test against channel statistics mismatches: We consider the robustness of the DNN detection by considering the CIR variation from offline training to online testing, as illustrated in Figure 9. We consider random variation in CIR at each receiver antenna, where σ^2_{var} denotes the percentage of the change of channel statistics from offline training to online testing, and 0% means no mismatch. We observe from Figure 9 that CIR variation does not degrade BER performance significantly.

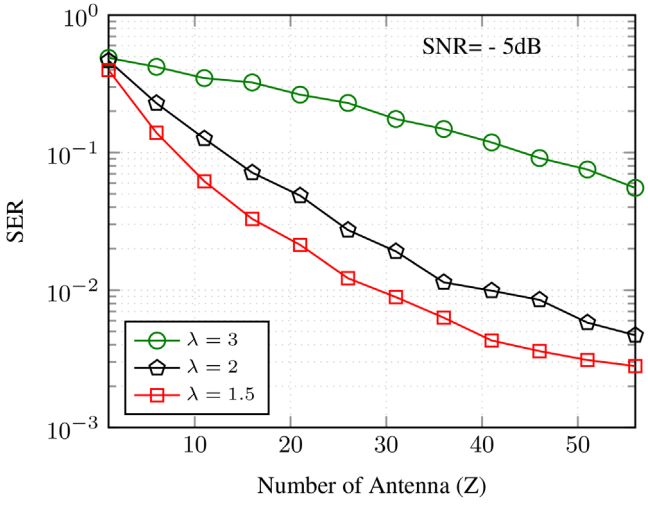

FIGURE 10 Impact of overloading factor λ and number of antennas Z in M-SCMA system

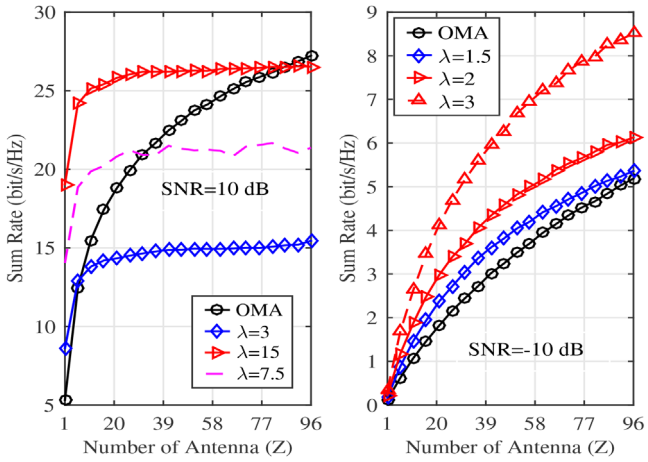

FIGURE 11 Sum rate versus number of antennas performance in M-SCMA

Furthermore, in Figure 10, we highlight the importance of number of antennas at the BS to achieve a higher overloading factor (λ) in M-SCMA system with MMPA detection. Array gain of M-SCMA allows to enhance the spectral efficiency of a wireless system with fixed SER, as observed in Figure 10. Therefore, massive antennas at the BS can significantly reduce the SER in an M-SCMA system.

4.3.3 | When does M-SCMA have better sum rate than OMA?

The sum rate $R_{\text{M-SCMA}}$ of multiplexed users in the M-SCMA system is analysed and is shown in Figure 11. The $R_{\text{M-SCMA}}$ is expressed as

$$R_{\mathrm{M-SCMA}} = \sum_{j=1}^{J}\left[\log_2\left(1+\frac{\sum_{\tilde{z}=1}^{Z} P_j||\mathrm{diag}\left(\mathbf{h}_{j,\tilde{z}}\right)\mathbf{x}_j||^2}{\sum_{\tilde{z}=1}^{Z}\sum_{i=\Omega,i\neq j} P_i||\mathrm{diag}\left(\mathbf{h}_{i,\tilde{z}}\right)\mathbf{x}_i||^2+N_0}\right)\right], \quad (17)$$

where Ω is the set of overlapping users with jth user on the $\tilde{k}$th resource. For example, second and third users share the same resource node 1 with user one (in Figure 3). Therefore, $\Omega = \{2, 3\}$ in (17) for the first resource node. The sum rate of the proposed M-SCMA system is shown in Figure 11. At high SNR (SNR=10 dB), OMA system sum rate increases exponentially as shown in Figure 11 (left) and crosses the M-SCMA's sum rate. Since M-SCMA system is interference limited.[3] However, M-SCMA can have a higher sum rate for a lower number of antennas than the OMA as observed in Figure 11 (left). Furthermore, M-SCMA's sum rate can also be enhanced by increasing the overloading factor in the system as shown in Figure 11 (left). Since large Z allows the user separation at the BS. Therefore, one should decide the overloading factor and number of antennas in M-SCMA to get a better sum rate than the OMA. Furthermore, at low SNR (SNR $= -10$ dB), M-SCMA has better sum rate than the OMA for all ranges of antennas, as observed in Figure 11 (right). Hence, in M-SCMA-based system, SNR level, number of antennas (Z), and overloading factor λ are essential parameters to decide the system sum rate, unlike the conventional OMA-based system.

5 | CONCLUSIONS

This paper proposed the uplink SCMA system with massive antennas at BS, and it is referred to as M-SCMA system. Furthermore, EMPA, MMMP, and DNN-based detection is proposed for M-SCMA system. Results show that array gain due to massive antennas can be used to improve the spectral and transmit power efficiency of the M-SCMA system. It is also shown that EMPA has better performance than MMPA due to detection gain with marginal increment in complexity. Performance and complexity of MMPA (with and without perfect channel information) and DNN is compared for the proposed M-SCMA. Results show that DNN-based detection is preferable over MMPA to avoid explicit channel estimation and reduces the detection complexity in the proposed M-SCMA system. The trade-off between SCMA and OMA in massive antenna system is investigated by analysing the sum rate for different values of overloading factor.

ORCID

Sanjeev Sharma https://orcid.org/0000-0001-7488-1064

[3] In (17), the sum rate of M-SCMA system is limited by the interference and noise levels. At high and low SNR, the sum rate is limited by mainly interference and noise level, respectively, as observed in (17).

REFERENCES

1. Dai, L., et al.: A survey of non-orthogonal multiple access for 5G. IEEE Commun. Surv. Tutorials 20(3), 2294–2323 (2018)
2. Guo, J., et al.: User pairing and power allocation for downlink non-orthogonal multiple access. In: IEEE Globecom Workshops (GC Wkshps), pp. 1–6 (2016)
3. Wang, F., et al.: Active user detection of uplink grant-free SCMA in frequency selective channel. In: IEEE 87th Vehicular Technology Conference (VTC Spring), pp. 1–6 (2018)
4. Vaezi, M., et al.: Multiple Access Techniques for 5G Wireless Networks and Beyond. Springer, Cham (2019)
5. Sharma, S., et al.: Joint power-domain and SCMA-based NOMA system for downlink in 5G and beyond. IEEE Commun. Lett. 23(6), 971–974 (2019)
6. Hosseini, H., et al.: Wavelet-based cognitive SCMA system for mmWave 5G communication networks. IET Commun. 11(6), 831–836 (2016)
7. Tang, S., et al.: Low complexity joint MPA detection for downlink MIMO-SCMA. In: IEEE Global Communications Conference (GLOBECOM), pp. 1–4 (2016)
8. Liu, L., et al.: Downlink MIMO in LTE-advanced: SU-MIMO vs. MU-MIMO. IEEE Commun. Mag. 50(2), 140–147 (2012)
9. Tang, W., et al.: Design of MIMO-PDMA in 5G mobile communication system. IET Commun. 14(1), 76–83 (2019)
10. Du, Y., et al.: Joint sparse graphdetector design for downlink MIMO-SCMA systems. IEEE Wireless Commun. Lett. 6(1), 14–17 (2016)
11. Higuchi, K., Kishiyama, Y.: Non-orthogonal access with random beamforming and intra-beam SIC for cellular MIMO downlink. In: IEEE 78th Vehicular Technology Conference (VTC Fall), pp. 1–5 (2013)
12. Yan, C., et al.: Downlink multiple input multiple output mixed sparse code multiple access for 5G system. IEEE Access 6, 20837–20847 (2018)
13. Cui, Q., Shuang, K.: Joint SCMA and waveform optimisation for WPDM-based logging cable telemetry systems under sampling clock offset. IET Commun. 13(3), 345–353 (2018)
14. Tian, L., et al.: A low complexity detector for downlink SCMA systems. IET Commun. 11(16), 2433–2439 (2017)
15. Lai, K., et al.: Simplified sparse code multiple access receiver by using truncated messages. IET Commun. 12(16), 1937–1945 (2018)
16. Sharma, S., et al.: SCMA codebook based on optimization of mutual information and shaping gain. In: IEEE Globecom Workshops (GC Wkshps), pp. 1–6 (2018)
17. Liu, T., et al.: Capacity for downlink massive MIMO MU-SCMA system. In: IEEE International Conference on Wireless Communications & Signal Processing (WCSP), pp. 1–5 (2015)
18. Pan, Z., et al.: Uplink spatial modulation SCMA system. IEEE Commun. Lett. 23(1), 184–187 (2018)
19. Pan, Z., et al.: Multi-dimensional space time block coding aided downlink MIMO-SCMA. IEEE Trans. Veh. Technol. 68(7), 6657–6669 (2019)
20. Chen, X., et al.: Exploiting multiple antenna techniques for non-orthogonal multiple access. IEEE J. Sel. Areas Commun. 35(10), 2207–2220 (2017)
21. Chi, Y., et al.: Practical MIMO-NOMA: Low complexity and capacity-approaching solution. IEEE Trans. Wireless Commun. 17(9), 6251–6264 (2018)
22. Kim, M., et al.: Deep learning-aided SCMA. IEEE Commun. Lett. 22(4), 720–723 (2018)
23. Abidi, I., et al.: Convolutional neural networks for blind decoding in sparse code multiple access. In: IEEE 15th International Wireless Communications & Mobile Computing Conference (IWCMC), pp. 2007–2012 (2019)
24. Parvez, S., et al.: On impact of imperfect CSI over hexagonal QAM for TAS/MRC-MIMO cooperative relay network. IEEE Commun. Lett. 23(10), 1721–1724 (2019)
25. Qin, Z., et al.: Deep learning in physical layer communications. IEEE Wireless Commun. 26(2), 93–99 (2019)
26. Ye, H., et al.: Power of deep learning for channel estimation and signal detection in OFDM systems. IEEE Wireless Commun. Lett. 7(1), 114–117 (2017)

27. Van Luong, T., et al.: Deep learning-based detector for OFDM-IM. IEEE Wireless Commun. Lett. 8(4), 1159–1162 (2019)
28. Simeone, O.: A very brief introduction to machine learning with applications to communication systems. IEEE Trans. Cognit. Commun. Networking 4(4), 648–664 (2018)
29. Sharma, M.K., et al.: Deep learning based online power control for large energy harvesting networks. In: IEEE International Conference on Acoustics, Speech and Signal Processing (ICASSP), pp. 8429–8433 (2019)
30. Sharma, S., Hong, Y.: UWB receiver via deep learning in MUI and ISI scenarios. IEEE Trans. Veh. Technol. 69(3), 3496–3499 (2020)
31. Savin, V.: Min-Max decoding for non binary LDPC codes. In: IEEE International Symposium on Information Theory, Toronto, ON, pp. 960–964 (2008)
32. Zhang, S., et al.: A capacity-based codebook design method for sparse code multiple access systems. In: IEEE International Conference on Wireless Communications & Signal Processing (WCSP), pp. 1–5 (2016)
33. Sharma, S., et al.: User activity detection-based large SCMA system for uplink grant-free access. In: IEEE International Conference on Communications Workshops (ICC Workshops), pp. 1–6 (2019)

How to cite this article: Sharma S, Deka K, Beferull-Lozano Baltasar. Low-complexity detection for uplink massive MIMO SCMA systems. *IET Commun.* 2021;15:51–59. https://doi.org/10.1049/cmu2.12057